First Pd@Organo−Si(HIPE) Open-Cell Hybrid Monoliths Generation Offering Cycling Heck Catalysis Reactions

Simona Ungureanu,[†,||] Hervé Deleuze,[‡] Clément Sanchez,[§] Marcel I. Popa,[||] and Rénal Backov*,[†]

Centre de Recherche Paul Pascal, UPR 8641-CNRS, Université Bordeaux 1, 115 Avenue Albert Schweitzer, 33600 Pessac, France, Université Bordeaux I/CNRS, Institut des Sciences Moléculaires (ISM), 351 Cours de la Libération, F 33405 Talence, France, Laboratoire de Chimie de la Matière Condensée de Paris, UMR-7574 CNRS, Université Pierre et Marie Curie, 4 Place Jussieu, 75000 France, and Facultatea de Inginerie Chimica si Protectia Mediului, B-dul D. Mangeron, nr. 71, Iasi, 700050, Romania

Received June 6, 2008. Revised Manuscript Received August 26, 2008

The syntheses and characterization of a new class of grafted organo−Si(HIPE) "high internal phase emulsion" open-cell matrixes is first proposed. Second, internal palladium particles heterogeneous nucleation is briefly discussed, leading finally to the generation of the new Pd@organo−Si(HIPE) series. The matrixes synthesized offer good turnovers and cycling performances For instance, the Pd@mercapto−Si(HIPE) matrix allows reaching at least 96% of Heck coupling catalysis yield during seven cycling tests. The Pd/iodobenzene molar ratio was settled at 0.004 and 0.002. The turnover number (TON) and turnover frequency (TOF) addressed with these new monolith catalysts are reaching values comparable with the ones obtained with powdered catalysts. Considering the fact that the catalysts in use are not powders but rather monoliths bearing hierarchical porosities, the series of Pd@organo−Si(HIPE) compounds combine heterogeneous catalysis efficiency and facile reusability where catalyzed species and catalyst supports can be easily separated by a simple removal of either the monolith or the solution from the reaction media.

Introduction

Recently, the novel concept of "integrative chemistry"[1] has emerged from the interface between bioinspired approaches,[2] general soft chemistry (including hybrid organic−inorganic chemistry,[3] organic polymer, and supramolecular chemistry), and complex fluids. In this approach, chemistry and process are strongly coupled. Through the application of this concept, the set of chemical expertise involved has to be strongly predictated in view of the final expected function. Current approaches to hierarchically organized inorganic materials include coupling of multiscale templating effects combining self-assembled surfactants with larger molds as emulsion droplets,[4] air−liquid foams,[5] latex beads,[6] and so forth. These templating modes could also be addressed while applying external stimuli.[7] More particularly, ordered macro−mesoporous materials are of interest for multiple applications in heterogeneous catalysis, separation techniques, absorption, sensors, optics, etc. One way of generating such architectures is to use either direct concentrated nonaqueous emulsions[8] or surfactant/colloids stabilized aqueous emulsions.[9,10] With this aim, we have developed a new process for obtaining macrocellular silica monoliths with a good control over the final macroscopic cell sizes and morphologies by tuning the oil volume fraction of the starting emulsion. This new series of silica porous networks were labeled Si(HIPE),[4b] in reference to the first generation of porous organic polymers obtained through the use of concentrated reverse emulsions, known under the poly-HIPE

* Corresponding author. E-mail: backov@crpp-bordeaux.cnrs.fr.
† Centre de Recherche Paul Pascal, UPR 8641-CNRS, Université Bordeaux 1.
‡ Université Bordeaux I/CNRS, Institut des Sciences Moléculaires.
§ Université Pierre et Marie Curie.
|| Facultatea de Inginerie Chimica si Protectia Mediului.

(1) (a) Backov, R. *Soft Mater.* **2006**, *2*, 452. (b) Prouzet, E.; Khani, Z.; Bertrand, M.; Tokumoto, M.; Gyuot-Ferreol, V.; Tranchant, J.-F. *Microporous Mesoporous Mater.* **2006**, *96*, 369. (c) Sanchez, C.; Boissière, C.; Grosso, D.; Laberty, C.; Nicole, L. *Chem. Mater.* **2008**, *3*, 682. (d) Prouzet, E.; Ravaine, S.; Sanchez, C.; Backov, R. *New J. Chem.* **2008**, *32*, 1284.
(2) (a) Ozin, G. A. *Chem Commun.* **2000**, *6*, 419. (b) Sanchez, C.; Arribart, H.; Giraud-Guille, M. M. *Nat. Mater.* **2005**, *4*, 277. (c) Xu, A.-W.; Ma, Y.; Cölfen, H. *J. Mater. Chem.* **2007**, *17*, 415.
(3) (a) Sanchez, C.; Ribot, F. *New J. Chem.* **1994**, *18*, 1007. (b) Sanchez, C.; Julian, B.; Belleville, P.; Popall, M. *J. Mater. Chem.* **2005**, *15*, 3559. (c) *Functional Hybrid Materials*; Gómez-Romero, P., Sanchez, C., Eds.; Wiley-VCH: Weinheim, Germany, 2003.
(4) (a) Imhof, A.; Pine, D. J. *Adv. Mater.* **1998**, *10*, 697. (b) Carn, F.; Colin, A.; Achard, M.-F.; Deleuze, H.; Birot, M.; Backov, R. *J. Mater. Chem.* **2004**, *14*, 1370.
(5) (a) Chandrappa, G. T.; Steunou, N.; Livage, J. *Nature* **2002**, *416*, 702. (b) Maekawa, H.; Esquena, J.; Bishop, S.; Solans, C.; Chmelka, B. F. *Adv. Mater.* **2003**, *15*, 591. (c) Walsh, D.; Kulak, A.; Aoki, K.; Ikoma, T.; Tanaka, J.; Mann, S. *Angew. Chem., Int. Ed.* **2004**, *43*, 6691. (d) Carn, F.; Steunou, N.; Colin, A.; Livage, J.; Backov, R. *Chem. Mater.* **2005**, *17*, 644. (e) Carn, F.; Masse, P.; Saadaoui, H.; Julián-López, B.; Deleuze, H.; Ravaine, S.; Sanchez, C.; Talham, D. R.; Backov, R. *Langmuir* **2006**, *22*, 5469.
(6) (a) Holland, B. T.; Blanford, C. F.; Stein, A. *Science* **1998**, *281*, 538. (b) Antonietti, M.; Berton, B.; Göltner, C.; Hentze, H.-P. *Adv. Mater.* **1998**, *10*, 154.
(7) (a) Busch, S.; Dolhaine, H.; DuChesne, A.; Heinz, S.; Hochrein, O.; Laeri, F.; Podebrad, O.; Vietze, U.; Weiland, T.; Kniep, R. *Eur. J. Inorg. Chem.* **1999**, *10*, 1643. (b) Leroy, C. M.; Achard, M.-F.; Babot, O.; Steunou, N.; Masse, P.; Livage, J.; Binet, L.; Brun, N.; Backov, R. *Chem. Mater.* **2007**, *19*, 3988. (c) Chronakis, I. S. *J. Mater. Process. Technol.* **2005**, *167*, 283.
(8) Imhof, A.; Pine, D. J. *Nature* **1997**, *389*, 948.
(9) Yi, G.-R.; Yang, S. M. *Chem. Mater.* **1999**, *11*, 2322.
(10) Binks, B. P. *Adv. Mater.* **2002**, *14*, 1824.

10.1021/cm801525c CCC: $40.75
Published on Web 09/30/2008

acronym (polymerized high internal phase emulsion).[11] More recently, taking benefit of the hybrid organic−inorganic chemistry versatility, we combined tetraethoxyorthosilane (TEOS) with diverse organically modified silanes (ORMOSILs) to generate the first series of organo−Si(HIPE) complex architectures bearing "molecular information",[12a] particularly the ability to stabilize palladium nanoparticles, whereas others have generated hybrid silsesquioxane hybrid poly-HIPE[12b,c] or poly-HIPE bearing metallic nanoparticles.[12d,e] Our group is focusing on palladium nanoparticles generation within organo−Si(HIPE) matrixes because palladium-catalyzed C−C bond formation, such as the Mizoroki−Heck,[13] Suzuki−Miyaura,[14] and Buchwald−Hartwig[15] reactions, provide efficient methods for assembling complex structures. Despite the remarkable versatility of Pd-based catalysts in organic synthesis, the difficulty to efficiently remove metal traces from the final organic products is appearing as a strong limitation for large-scale applications. A common approach to circumvent this issue is heterogeneous catalysis.[16] In this way, palladium nanoparticles will be supported on a matrix such as carbon,[17a] ordered[17b] or amorphous silicates,[17c] zeolites,[17d] or poly-HIPE.[17e] In order to stabilize as far as possible the nucleated particles in its zero-valent state, support surfaces might be functionalized with ligands such as phosphines,[18] carbenes,[19] pincer ligands,[20] palladacycles,[21] and so forth.

In this general context, we first propose herein the synthesis and characterization of a new class of grafted "*g*-organo−Si(HIPE)" open-cell matrixes followed by internal palladium particles heterogeneous nucleation, leading second to the generation of the new Pd@organo−Si(HIPE) series. Finally, these supported catalysts have been tested toward the Mizoroki−Heck coupling reaction and demonstrate good performances.

Results and Discussion

The final hybrid macrocellular foams should possess the ability to efficiently anchor and stabilize palladium metallic nanoparticles. In this issue, organically modified silanes bearing amino or mercapto groups, known to be efficient for this application, have been chosen. The selected precursors were the 3-aminopropyltrimethoxysilane and the 3-mercaptopropyltrimethoxysilane. Cocondensation synthesis of the hybrid mercapto−Si(HIPE) open-cell monoliths have been published elsewhere as well as its characterization at diverse length scales.[12a] This previous study demonstrated that the surfactant used to both stabilize the direct emulsion and induce the compounds texturation at the mesoscale level was partially retained within the frameworks despite a severe washing process.[12a] This is the reason why we present herein an alternative method based on a two-step process: first the generation of native Si(HIPE) supports[4b] followed by surface grafting of the selected silane derivative precursors (see the Experimental Section for the detailed synthetic routes). Hybrid matrixes obtained through this grafting synthetic pathway will be called hereafter *g*-mercapto−Si(HIPE) or *g*-amino−Si(HIPE). Grafted samples have been characterized by scanning electron microscopy (SEM), transmission electron microscopy (TEM), mercury porosimetry, nitrogen adsorption isotherms, and small-angle X-ray scattering (SAXS).

The macroscopic texture of the grafted monoliths as observed through SEM (Figure 1a) remains intact after the grafting process and preserves the typical "hollow spheres" aggregation structure of the native Si(HIPE).[4b]

The interconnection size distribution (the size of the windows connecting two adjacent cells), as measured by mercury intrusion porosimetry, depicts a polydisperse distribution ranging from 10 up to 6000 nm, associated with two main contributions centered at 150 and 700 nm (0.7 μm) for *g*-amino−Si(HIPE) and 60 and 4000 nm (4 μm) for *g*-mercapto−Si(HIPE), respectively. In both cases some porosity is observed at 10 nm (Figure 2).

Specific morphological characterization (porosity, bulk, and skeleton densities) of these hybrid compounds can be found in Table 1. Here, as was the case with earlier either Si(HIPE)[4b] or organo−Si(HIPE)[12a] compounds it is important to note that the mechanical properties of the materials presented herein are high enough to endure mercury porosimetry.

At the mesoscopic length scale, nitrogen gas sorption/desorption isotherms have been recorded (Figure 3). Specific surface area and pore size distribution were estimated according the BET and BJH methods (Table 2). Both specific surface area and pore volume were found to decrease drastically upon modification, as expected from the reduction of the void space due to the presence of grafted organic

(11) (a) Barby, D.; Haq, Z. European Patent 0060138, 1982. (b) Cameron, N. R.; Sherrington, D. C. High internal phase emulsions (HIPEs) Structure, properties and use in polymer preparation. *Advances in Polymer Science*; Springer: Berlin/Heidelberg, 1996; Vol. 126, p 163. (c) Cameron, N. *Polymer* **2005**, *46*, 1439. (d) Zhang, H.; Cooper, A. I. *Soft Matter* **2005**, *2*, 107.
(12) (a) Ungureanu, S.; Birot, M.; Laurent, G.; Deleuze, H.; Babot, O.; Julián-López, B.; Achard, M.-F.; Popa, M. I.; Sanchez, C.; Backov, R. *Chem. Mater.* **2007**, *19*, 5786. (b) Normatov, J.; Silverstein, M. S. *Macromolecules* **2007**, *23*, 8329. (c) Normatov, J.; Silverstein, M. S. *Chem. Mater.* **2008**, *4*, 1571. (d) Zhang, H.; Hussain, I.; Brust, M.; Cooper, A. I. *Chem. Commun.* **2006**, *24*, 2539. (e) Zhang, H.; Hardy, G. C.; Khimyak, Y. Z.; Rosseinsky, M. J.; Cooper, A. I. *Chem. Mater.* **2004**, *16*, 4245.
(13) (a) Mizoroki, T.; Mori, K.; Ozaki, A. *Bull. Chem. Soc. Jpn.* **1971**, *44*, 581. (b) Heck, R. F.; Nolley, J. P. *J. Org. Chem.* **1972**, *37*, 2320.
(14) Miyaura, N.; Suzuki, A. *Chem. Rev.* **1995**, *95*, 2457.
(15) (a) Culkin, D. A.; Hartwig, J. F. *Acc. Chem. Res.* **2003**, *36*, 234. (b) Muci, A. R.; Buchwald, S. L. *Top. Curr. Chem.* **2002**, *219*, 131.
(16) For reviews of heterogeneous Pd catalysts, see: (a) Blaser, H.-U.; Indolese, A.; Schnyder, A.; Steiner, H.; Studer, M. *J. Mol. Catal. A: Chem.* **2001**, *173*, 3. (b) Dantas Ramos, A. L.; da Silva Alves, P.; Aranda, D. A. G.; Schmal, M. *Appl. Catal., A* **2004**, *277*, 71.
(17) (a) Mehnert, C. P.; Ying, J. Y. *Chem. Commun.* **1997**, 2215. (b) Mehnert, C. P.; Weaver, D. W.; Ying, J. Y. *J. Am. Chem. Soc.* **1998**, *120*, 12289. (c) Richmond, M. K.; Scott, S. L.; Alper, H. *J. Am. Chem. Soc.* **2001**, *123*, 10521. (d) Okumura, K.; Nota, K.; Yoshida, K.; Niwa, M. *J. Catal.* **2005**, *231*, 245. (e) Desforges, A.; Deleuze, H.; Mondain-Monval, O.; Backov, R. *Ind. Eng. Chem. Res.* **2005**, *44*, 8521.
(18) (a) Leadbeater, N. E.; Marco, M. *Chem. Rev.* **2002**, *102*, 3217. (b) McNamara, C. A.; Dixon, M. J.; Bradley, M. *Chem. Rev.* **2002**, *102*, 3275. (c) Desforges, A.; Backov, R.; Deleuze, H.; Mondain-Monval, O. *Adv. Funct. Mater.* **2005**, *15*, 1689.
(19) Mayr, M.; Buchmeiser, M. R.; Wurst, K. *Adv. Synth. Catal.* **2002**, *344*, 712.
(20) (a) Herrmann, W. A.; Brossmer, C.; Oefele, K.; Reisinger, C.-P.; Priermeier, T.; Beller, M.; Fischer, H. *Angew. Chem., Int. Ed. Engl.* **1995**, *34*, 1844. (b) Beller, M.; Fischer, H.; Herrmann, W. A.; Oefele, K.; Brossmer, C. *Angew. Chem., Int. Ed. Engl.* **1995**, *34*, 1848.
(21) (a) Baleizão, C.; Corma, A.; García, H.; Leyva, A. *Chem. Commun.* **2003**, 606. (b) Baleizão, C.; Corma, A.; García, H.; Leyva, A. *J. Org. Chem.* **2004**, *69*, 439.

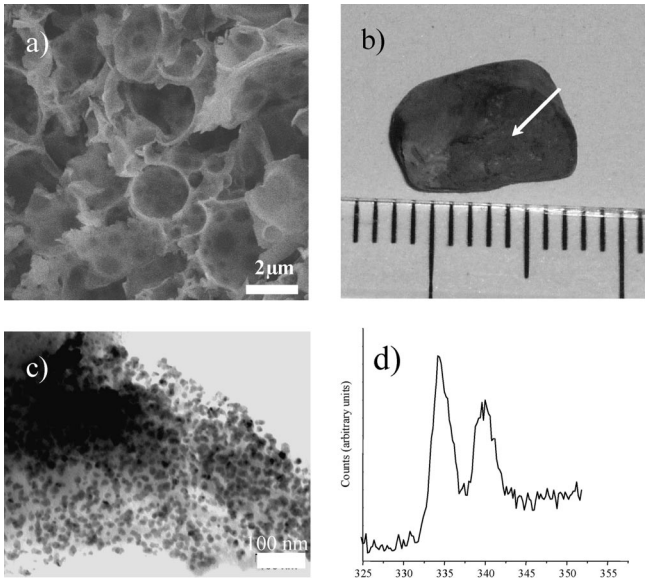

Figure 1. (a) Textural macroporosity observed through scanning electron microscopy (SEM). (b) Typical monolith after the Pd nanoparticles heterogeneous nucleation (the white arrow indicates the monolith inner part). (c) Pd nanoparticles observed through transmission electron microscopy (TEM). (d) Typical X-ray photoelectron spectroscopy (XPS) performed on the Pd@organo−Si(HIPE) compounds, focused on the bands centered at 335 and 340.8 eV that correspond, respectively, to the Pd $3d_{5/2}$ and $3d_{3/2}$.

moieties on the inner surface of the pores. For the *g*-amino−Si(HIPE) monolith, the observation of a hysteresis loop on the isotherm diagram clearly indicates the presence of mesoporosity and the upturn at p/p_0 close to 1.0 is an indication of some textural macroporosity, also identified by Hg porosimetry.

Porosity distribution provided by the density functional theory (DFT) calculation depicts pore widths ranging and decreasing in intensity from 1.1 to 3 nm describing both micro- and mesoporosity (Figure 3). A weak hysteresis loop can be observed between the adsorption and desorption curves for *g*-mercapto−Si(HIPE) sample which is an indication that the hybrid compound is bearing essentially a microporous structure (pore sizes between 0.7 and 1.5 nm, as estimated by DFT) associated with some residual mesoporosity (pore sizes higher than 1.5 nm). Transmission electron microscopy exhibits disordered worm-hole mesoporous morphology supported by SAXS profiles (Figure 4).

Both materials show a large peak centered at 0.18 $Å^{-1}$ (3.5 nm), a strong indication of the presence of vermicular mesoporosity without any long-range ordering.[4b] Considering both the SAXS and nitrogen physisorption measurements there is, at first glance, a certain discrepancy when considering the results. The nitrogen physisorption measurement mostly describes a microporous character, weakly mesoporous for the *g*-amino−Si(HIPE) compound, but does not provide strong evidence for high population of 2.5 nm pore diameters (3.5 nm minus 1 nm of wall thickness). In fact we have to take into account the length (≈6 Å) of the silane derivatives in use to functionalize the Si(HIPE) that will lower the mesopore diameters but will not be seen by SAXS. If we consider the SAXS result (3.5 nm, that corresponds to the wall-to-wall distance) and retain 2 times the organically modified silanes length (1.2 nm) and the silica wall thickness

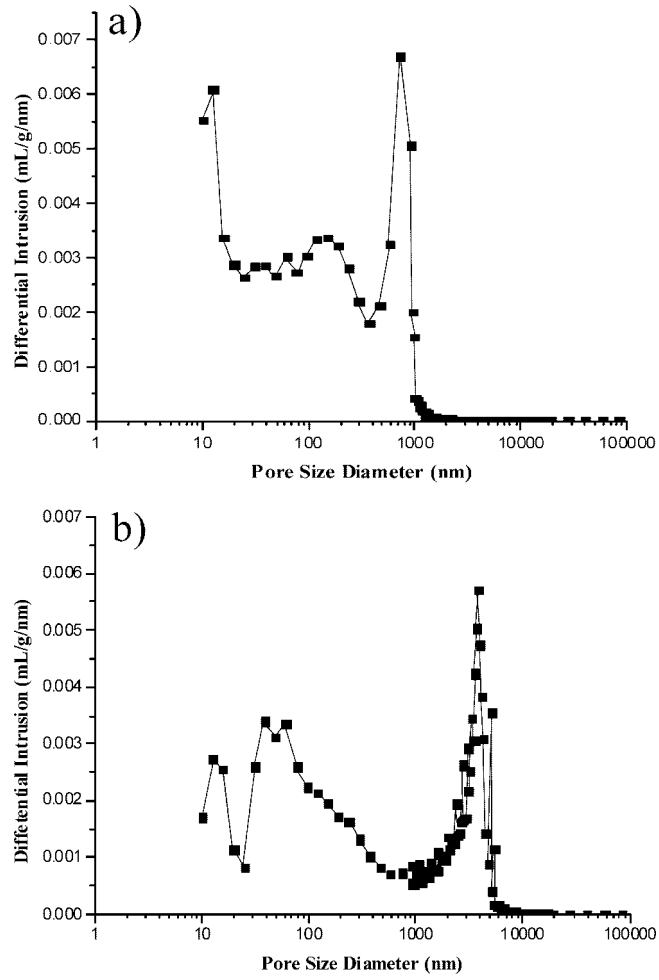

Figure 2. Macroscopic pore size distributions obtained through mercury intrusion porosimetry: (a) *g*-amino−Si(HIPE); (b) *g*-mercapto−Si(HIPE).

Table 1. Hg Porosimetry Characteristics of the Supported Catalysts

samples	*g*-amino−Si(HIPE)	*g*-mercapto−Si(HIPE)
intrusion volume ($cm^3 \cdot g^{-1}$)	8.8	10.7
porosity (%)	88	92
bulk density ($g \cdot cm^{-3}$)	0.14	0.1
skeletal density ($g \cdot cm^{-3}$)	1.13	1.1

(1 nm), we recover 1.1 nm of pore diameters in good agreement with the nitrogen physisorption measurements.

Finally, the organic contents of this monolith series have been quantified using thermogravimetric analysis (TGA). The associated stoichiometries are listed in Table 3.

Palladium heterogeneous nucleation within the organo−Si(HIPE) materials has been performed. The route chosen was the in situ $Pd(OAc)_2$ reduction using $NaBH_4$ in a THF/H_2O (50/50 v/v) mixture in the presence of triphenylphosphine (PPh_3) as a zero-valent state nanoparticles stabilizing agent[18] (4/1 PPh_3/Pd ratio) (see the Experimental Section for all the detailed synthetic routes). The resulting supported catalysts were called Pd@*g*-amino−Si(HIPE), Pd@*g*-mercapto−Si(HIPE), and Pd@mercapto−Si(HIPE) depending on the starting organo−Si(HIPE) material employed. Upon the synthetic route in use, it was observed that the monoliths, originally white, become homogeneously black from the

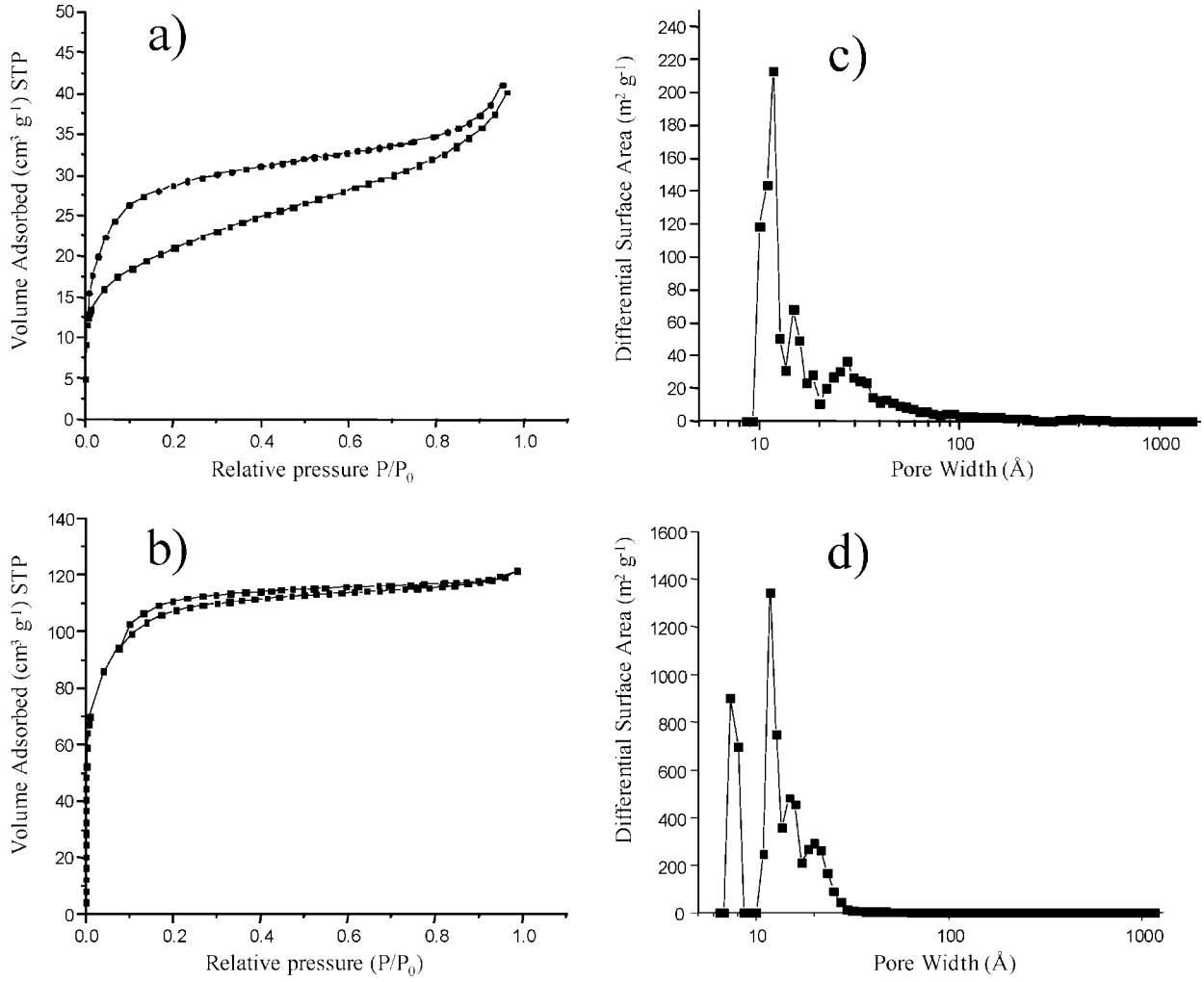

Figure 3. Nitrogen adsorption−desorption curves: (a) *g*-amino−Si(HIPE); (b) *g*-mercapto−Si(HIPE). Mesoscopic and microscopic pore size distributions obtained through the differential functional theory (DFT): (c) *g*-amino−Si(HIPE); (d) *g*-mercapto−Si(HIPE).

Table 2. Specific Surface Area of the Catalysts Obtained through N_2 Adsorption/Desorption Physisorption Experiments

samples	native Si(HIPE)	*g*-amino− Si(HIPE)	*g*-mercapto− Si(HIPE)
specific surface area ($m^2 \cdot g^{-1}$)[a]	730[b]	300	400
specific surface area ($m^2 \cdot g^{-1}$)[c]	220[b]	150	70
total pore volume ($cm^3 \cdot g^{-1}$)	0.35[b]	0.15	0.2

[a] According to the BET model. [b] Data extracted from ref 4b. The BET method describes both microporosity and mesoporosity, whereas the BJH method has been applied only to pore diameters higher than 1.5 nm that characterize the materials mesoporosity. [c] According to the BJH model.

outer to the inner part of the monoliths (Figure 1b). This feature is an indication that Pd nanoparticles have been macroscopically homogeneously nucleated within the organo−Si(HIPE) compounds. Figure 1c shows that the nanoparticles have been generated, with average size diameters around 5−10 nm. At that point, by considering the data that concerns the materials micro−mesoporosity ranging from 1.1 to 3 nm at best, we are obliged to consider that the nanoparticles seen in Figure 1c are not trapped within the materials' micro- or mesoporosity but are rather disposed at their outer surface and are just covering the materials' internal macroporosity (coming from the oil droplets' removal). This feature is of importance as all the results concerning the upcoming catalysis will be addressed with nanoparticles present at the

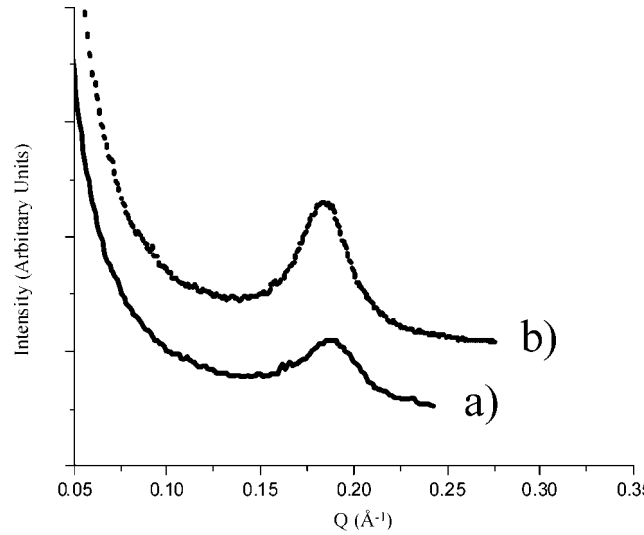

Figure 4. Small-angle X-ray scattering profiles: (a) *g*-amino−Si(HIPE); (b) *g*-mercapto−Si(HIPE).

internal surface of the materials' macropores only. Concerning the metallic character of the nucleated particles, previous work, concerning Pd heterogeneous nucleation within non-functionalized organic poly-HIPEs,[17e] has shown that the generated particles were in fact composed of a thin shell of

Scheme 1. (a) Expression of the Mizoroki−Heck Coupling Reaction between the Starting Iodobenzene and Styrene and (b) Typical Reactor in Use for the Catalysis Reactions

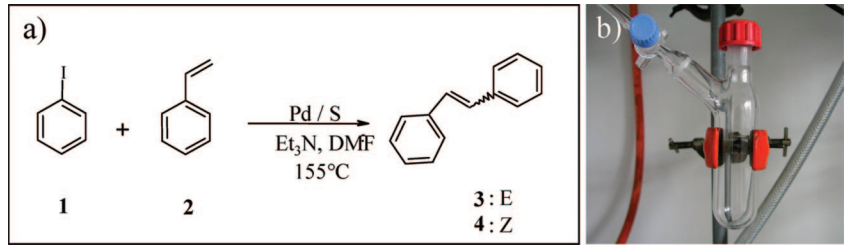

Table 3. Thermogravimetric Analysis and Associated Stoichiometries[a]

samples	organic weight loss %[b]	water weight loss%[b]	stoichiometry
g-amino−Si(HIPE)	9.5 (9.5)	8.03 (8)	$SiO_{1.946}(C_3H_8N)_{0.054}\cdot 2.96H_2O$
g-mercapto−Si(HIPE)	13.26 (13.25)	2.7 (2.7)	$SiO_{1.804}(C_3H_7S)_{0.196}\cdot 0.8H_2O$
mercapto−Si(HIPE)[c]	28.27 (28.20)	1.2 (1.24)	$SiO_{1.894}(C_3H_7S)_{0.106}(C_{17}H_{38}BrN)_{0.047}\cdot 0.058\ H_2O$

[a] Materials were calcined at 650 °C for 6 h with a first plateau at 200 °C for 2 h. The increase temperature was set to 2 °C/min, while the cooling temperature was driven by the oven inertia. [b] Weight loss extract from TGA. [c] The nongrafted compounds stoichiometries have been obtained by crossing TGA, CHN elemental analyses, and ^{29}Si experiments (ref 12a).

palladium oxide surrounding a Pd zero-valent core. In fact, if nonstabilized Pd nanoparticles are good enough for operating under reducing atmosphere, especially for heterogeneous hydrogenation catalysis reactions,[17e] their capability to promote good catalytic yields under oxidative conditions is minimized and needs a combination of matrixes stabilization, using entities bearing amino or mercapto groups, and the addition of, for instance, triphenylphosphine as a costabilizing agent.[18] Herein, the XPS spectrum of the grafted Pd shows two main peaks, centered at 335 and 340.8 eV (Figure 1d), respectively, corresponding to the $3d_{5/2}$ and $3d_{3/2}$ of metallic zero-valent Pd nanoparticles[22] (Figure 1d). The Pd (wt %) loading was 3.9%, 4.1%, and 3.9% for Pd@*g*-amino−Si(HIPE), Pd@*g*-mercapto−Si(HIPE), and Pd@mercapto−Si(HIPE), respectively, as estimated by elemental analysis.

Palladium supported monoliths were then used as catalysts for the Mizoroki−Heck coupling reaction between iodobenzene **1** and styrene **2** using triethylamine as a base and DMF as solvent, as expressed with the Scheme 1. The reactions were performed at 155 °C in a closed reactor with a lateral frit (Scheme 1b). Conversions of styrene (**2**) and iodobenzene (**1**) in (*E* + *Z*) stilbene (3 + 4) were followed by gas-phase chromatography (GPC).

Each of the batch experiments was conducted for 3 h, then the liquid medium was filtered, and a new reactive mixture was added to the remaining supported catalyst in order to perform a new catalytic run (Figure 4). The Pd/iodobenzene molar ratio was settled at 0.004 and 0.002. The first comment refers to the high selectivity observed in all cases for the *E* product isomer (*E*/*Z*: 96/4). Considering kinetics reported in Figure 5, all catalysts tested behave similarly on the first use, conversion being close to completion in all cases after 3 h.

However, under recycling, supported catalysts bearing a mercapto group appear to be less sensitive to deactivation/leaching than those functionalized with an amino group. For instance, mercapto derivatives are still active on the seventh

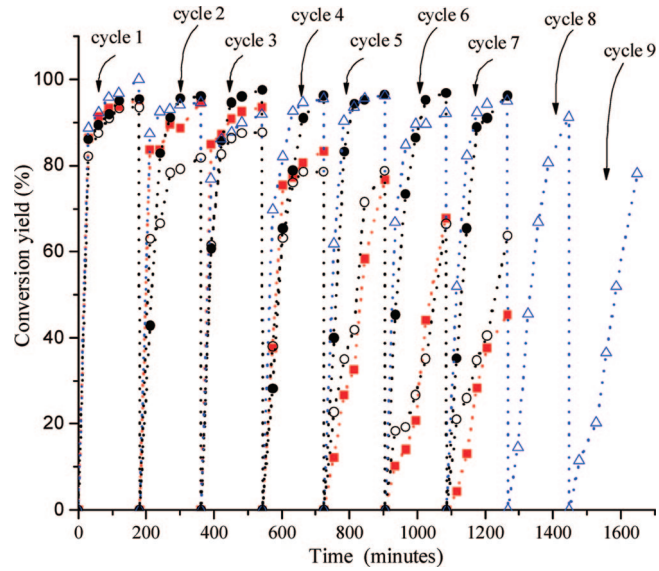

Figure 5. Cycling Heck coupling reactions and conversion yields: ■ Pd@*g*-amino−Si(HIPE); ● Pd@*g*-mercapto−Si(HIPE); △ Pd@mercapto−Si(HIPE); ○ Pd@*g*-amino−Si(HIPE), in this case, 0.055 g of support was used instead of the 0.11 g used for all the other tests. Conversion yields are the average of two GPC analyses.

cycle bearing a conversion yield of 97%. These results seem to confirm the previously reported observation that a mesoporous silica modified with a mercapto-propyl group provides a fairly good scavenging power toward Pd nanoparticles, thus reducing as far as possible Pd leaching in heterogeneous catalysis of the Mizoroki−Heck reaction.[23] Furthermore, in order to investigate the limits of these monolith catalysts toward their cycling performance, runs were pursued with Pd@mercapto−Si(HIPE) support, showing a slow decreases in conversion yield from 92% to 75% for the eight and ninth run, respectively. In order to further explore the catalytic properties of these hybrid materials limiting the Pd content, a new run of catalytic cycling was performed using Pd@*g*-amino−Si(HIPE) support where the Pd/iodobenzene molar

(22) Brun, M.; Berthet, A.; Bertolini, J. C. *J. Electron Microsc. Relat. Phenom.* **1999**, *104*, 55.

(23) Aksin, O.; Turkmen, H.; Artok, L.; Cetinkaya, B.; Chaoyinj, N.; Buyukgungor, O.; Ozkal, E. *J. Organomet. Chem.* **2006**, *691*, 30227.

Table 4. M−H Reaction of Iodobenzene with Styrene over Different Catalysts Synthesized

samples	TON	TOF (h^{-1})
g-amino−Si(HIPE)[a]	1300	62
g-amino−Si(HIPE)[b]	2961	141
g-mercapto−Si(HIPE)[a]	1409	78
mercapto−Si(HIPE)[a]	2783	103

[a] Using a 0.004 Pd/iodobenzene molar ratio. [b] Using a 0.002 Pd/iodobenzene molar ratio.

ratio was decreased to 0.002 (instead of 0.004) (Figure 5). Corresponding turnover numbers (TON) and turnover frequencies (TOF) have been calculated and are reported in Table 4.

The values obtained, in the good average for heterogeneous catalysis of Mizoroki−Heck reaction performed with powdered compounds,[23] are reaching the best results for silica-based supports, considering the work from Crudden et al.[24] Despite this good performance, it can be noticed that, in any case, the conversion yield, being constant to a high level in the first runs, slowly decreases after seven cycles. These observations suggest that the grafted hybrid derivatives allow some Pd leaching while performing cycling catalysis. In fact, palladium content analysis of the reaction media after each cycle using Pd@*g*-amino−Si(HIPE) (0.002 Pd/iodobenzene molar ratio) confirms this assumption: 3.5, 3.5, 4, 5, and 15 ppm of Pd were detected in solution after cycle 1 to cycle 5, respectively. The literature dealing with Mizoroki−Heck catalyzed reaction has clearly established that, in most cases, heterogeneous catalysts are merely reservoirs for highly active soluble forms of Pd[25] from where the metal can be leached in solution to perform an homogeneous catalysis. Pd leached in solution is considered to reprecipitate on the support surface after completion of the reaction.[26] The final slow activity decrease of the support after several reuses arises from successive Pd loss by solution leaching in each cycle of the run coming from the insufficient ability of the soluble Pd species to reintegrate in the support macroporosity at the end of the reaction.

Also we have had previously demonstrated that Au@poly-HIPE macroporous compounds were able to catalyze eosin reduction[27] while herein we demonstrate that Pd supported at the macroporous internal surface of hybrid compounds can repetitively catalyze Mizoroki−Heck coupling reactions. These results demonstrate that, to reach decent heterogeneous catalysis performances, highly mesoporous materials are not of crucial importance, this for two main reasons. One, if nanoparticles are nucleated within mesopores then one has to trigger for their accessibility during the catalysis reaction. Second, considering the fluid hydrodynamics within macroporous media, particularly for solvent (Newtonian fluid) associated with a Poiseuille flow bearing reactive species, the overall fluid flow will be driven by the Darcy's law,[28a,b] and the speed of the Poiseuille flow is decreasing from the center of the macropores to their surface (Scheme 2).

Scheme 2. Overall Hydrodynamic of a Newtonian Fluid (Solvent) Flowing within a Macropore[a]

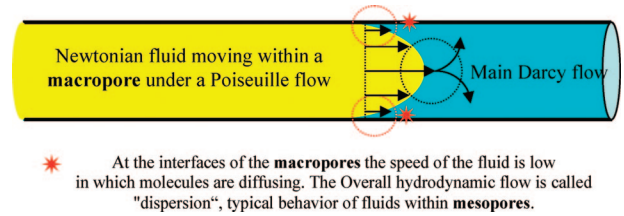

[a] The straight black arrows are representing the gradient of the fluid's speeds within a macropore.

Thereby, at the macropore surface, the flow speed will be equal to zero, where only reactive species will diffuse driven by the Fick equation. In the region close to the macropore surface, the overall scenario is a solvent moving with a weak speed in which reactive species are diffusing; this is a dispersion phenomenon,[28c] i.e., exactly the case of what occurs within mesopores.[28a,b] This behavior that certainly occurs close to the macropores interface is offering the double advantage of reactive species fast provisioning addressed with fast removal of the new synthesized molecules.

Conclusion

New hybrid Pd@*g*-organo−Si(HIPE) macrocellular foams have been synthesized. Considering the application, the Pd@mercapto−Si(HIPE) hybrid matrixes presented in this work are offering good yields, turnover, and cycling performances as reached with porous monolith-type compounds and not powders. Particularly, the Pd@mercapto−Si(HIPE) matrix allows reaching at least 96% of Heck coupling catalysis yield during seven cycling tests. Maybe more importantly, this work is also announcing the emergence of the use of macroporous materials when dealing with heterogeneous catalysis, as the diffusion-induced low speed is circumvented by the continuous macropore's high-speed flow inherent to the associated fluid hydrodynamic.

On the other hand, efforts need to be performed still toward minimizing the leaching process mentioned above and also catalysis reactions have to be addressed with less active aryl halides as bromides or chlorides. Considering the fact that the catalysts in use are not powders, but rather monoliths bearing macroporosities, the new series of Pd@organo−Si(HIPE) compounds should also find application in continuous flow devices.[29]

(24) Cruddden, C. M.; Satteesh, M.; Lewis, R. *J. Am. Chem. Soc.* **2005**, *127*, 10045.
(25) (a) Rocaboy, C.; Gladysz, J. A. *New J. Chem.* **2003**, *27*, 39. (b) Hartung, C. G.; Köhler, K. M.; Beller, M. *Org. Lett.* **1999**, *1*, 709. (c) Katayama, H.; Nagao, M.; Ozawa, F.; Ikegami, M.; Arai, T. *J. Org. Chem.* **2006**, *71*, 2699.
(26) (a) Corma, A.; Das, D.; García, H.; Leyva, A. *J. Catal.* **2005**, *229*, 322. (b) Rocaboy, C.; Gladysz, J. A. *Org. Lett.* **2002**, *4*, 1993. (c) Bergbreiter, D. E.; Osburn, P. L.; Frels, J. D. *Adv. Synth. Catal.* **2005**, *347*, 172. (d) Yu, K.; Sommer, W.; Weck, M.; Jones, C. W. *Adv. Synth. Catal.* **2005**, *347*, 161. (e) Cassol, C. C.; Umpierre, A. P.; Machado, G.; Wolke, S. I.; Dupont, J. *J. Am. Chem. Soc.* **2005**, *127*, 3298.
(27) Féral-Martin, C.; Birot, M.; Deleuze, H.; Desforges, A.; Backov, R. *React. Funct. Polym.* **2007**, *67*, 1072.
(28) (a) Coats, K. H.; Smith, B. D. *Soc. Pet. Eng. J.* **1964**, *131*, 73. (b) Levitz, P. In *Handbook of Porous Media*; Schuth, F., Sing, K., Weitkamp, J., Eds.; Wiley-VCH, 2002; p 37. (c) Guyon, E.; Hulin, J. P.; Petit, L.; Mitescu, C. D. In *Physical Hydrodynamics*; Oxford University Press, 2001.
(29) Nikbin, N.; Ladlow, M.; Ley, S. V. *Org. Process Res. Dev.* **2007**, *11*, 458.

Experimental Section

Chemicals. Tetraethylorthosilane (TEOS), tetradecyltrimethylammonium bromide (TTAB), *N*,*N*-dimethylformamide (DMF), (99%), and dodecane have been purchased from Fluka. (3-Mercaptopropyl)trimethoxysilane, 95%, was purchased from Lancaster. Sodium borohydride ($NaBH_4$), dodecane, and (2-amino)triphenilphosphine were purchased from Aldrich. Palladium tetrachloropalladate, tetrahydrofuran (99%), styrene (99%), and triethylamine (99%) were purchased from Acros Organics. Iodobenzene (98%) was purchased from Avocado. The reactants were used as received without further purification.

Instrumentation. Transmission electron microscopy was performed using a Hitachi H7650 TEM operating at 80 kV equipped with an Orius Gatan (11MPX) camera. Sample preparation was performed by first polymerizing an epoxy resin inside the organo-HIPE matrix and then cutting thin films, approximately 80 nm thick, using a Reichert-Jung Ultracut E. Scanning electron microscopy observations were performed with a Jeol JSM-840A SEM operating at 10 kV. The specimens were gold-coated or carbon-coated prior to examination. Surface areas and pore characteristics at the meso scale were obtained through nitrogen adsorption−desorption experiments using a Micromeritics ASAP 2010. Intrusion/extrusion mercury measurements were performed using a Micromeritics Autopore IV apparatus in order to assess the scaffolds' macrocellular cells characteristics. X-ray photoelectron spectroscopy experiments were performed using Escalab VG 220i XL apparatus. Small-angle X-ray scattering experiments were carried on a 18 kW rotating anode X-ray source (Rigaku-200) with use of a Ge (111) crystal as monochromator. The scattered radiation was collected on a two-dimensional detector (Imaging Plate system from Mar Research, Hamburg). The sample−detector distance was 500 mm. Thermogravimetric analyses were carried out under an oxygen flux (5 $cm^3 \cdot min^{-1}$) using a heating rate of 5 $°C \cdot min^{-1}$. The apparatus is a Stearam TAG-1750 thermogravimetric analyzer. Chromatography experiments were performed using a Varian 3800 and the Star chromatography software. The capillary column was a DB5 (5% phenyl groups) column. The IDB conversion was calculated from the peak area ratio of IDB relative to D (dodecane) as obtained from GC analysis.

Monolith Syntheses. *Synthesis of Native Si(HIPE).* TEOS (5.02 g) was added to aqueous solution of TTAB (16.02 g). Then, a concentrated hydrochloric acid solution (37%) was added (5.88 g). The aqueous phase was stirred for approximately 5 min in order to perform TEOS hydrolysis. Then the emulsion was prepared manually in a mortar by including dodecane drop by drop (40.05 g). The emulsion was transposed into a canister and left to age for 3 days at room temperature. The resulting material was washed with THF, dried in air, and calcined at 650 °C for 6 h (heating rate of 2 °C/min with a first plateau at 200 °C for 2 h). Specific surface area (BET) = 725 m^2/g.

Synthesis of Grafted Functionalized Si(HIPE) Supports. A piece of native Si(HIPE), (1 g) was added to a solution of 3-aminopropyltrimethoxysilane (2.3 g, 0.01 mol) or 3-mercaptopropyltrimethoxysilane (2.2 g, 0.01 mol) in chloroform (120 g). The suspension was placed under vacuum for a good impregnation (2−3 min) until the effervescence stopped. After 24 h aging at room temperature, the solution was filtered; the monoliths were then washed with chloroform and acetone and dried in air. The resulting monoliths are called *g*-amino−Si(HIPE) and *g*-mercapto−Si(HIPE).

Synthesis of Functionalized Si(HIPE) by Cocondensation Reaction. This cocondensation reaction has been published elsewhere.[12] The as synthesized monolith is called mercapto−Si(HIPE).

Catalyst Preparations. An amount of 1 g of functionalized support was immersed in a palladium acetate solution (0.33 g, 1.5×10^{-3} mol) containing triphenylphosphine (1.57 g, 6×10^{-3} mol) in THF (30 mL). The solution was left in the dark for 2 days. A fresh solution was prepared by dissolving $NaBH_4$ (0.567 g, 0.015 mol) in THF/H_2O (v/v, 30 mL) (dissolved oxygen was removed from water by argon bubbling (for 30 min). This mixture was quickly added to the metallic precursor solution under stirring, which resulted in a rapid color change from yellow to black and complete reduction within 1 h. All the matrixes were then washed in ethanol for 2 days until the washings were colorless and then dried overnight in air at room temperature before use. Final catalysts compound will be called Pd@*g*-amino−Si(HIPE), Pd@*g*-mercapto−Si(HIPE), and Pd@mercapto−Si(HIPE).

Catalytic Tests. A solution of iodobenzene **1** (10 mmol, 2.04 g), styrene **2** (15 mmol, 1.56 g), triethylamine (NEt_3) (11 mmol, 1.11 g), dodecane (5 mmol, 0.85 g as a GC internal standard) in DMF (10 mL), and the catalyst supports were placed in a glass pressure tube with a side-armed frit. Typically, 0.10 g of Pd@*g*-mercapto−Si(HIPE), 0.10 g of Pd@mercapto−Si(HIPE), and 0.11 g of Pd@*g*-amino−Si(HIPE) were used. The reaction mixture was gently purged with argon for 10 min, and then the reactor was immersed into a preheated oil bath at 155 °C, without stirring. Aliquots were periodically withdrawn from the reaction mixture and diluted with 1.0 mL of ice-cooled THF before the GC analysis.

Recycling Tests. After running the reaction between **1** and **2** according to the general reaction procedure described above, the liquid phase was withdrawn from the reactor, under Ar, through the frit, and a fresh mixture of reagents, base, and solvent was added to the remaining support in order to perform a new catalytic cycle.

CM801525C